

MEASUREMENT OF AIRFOIL HEAT TRANSFER  
COEFFICIENTS ON A TURBINE STAGE

Robert P. Dring  
Michael F. Blair  
United Technologies Research Center

## INTRODUCTION

The primary basis for heat transfer analysis of turbine airfoils is experimental data obtained in linear cascades. These data have been very valuable in identifying the major heat transfer and fluid flow features of a turbine airfoil. The question of major interest is how well all of these data translate to the rotating turbine stage. It is known from the work of Lokay and Trushin (ref. 1) that average heat transfer coefficients on the rotor may be as much as 40 percent above the values measured on the same blades non-rotating. Recent work by Dunn and Holt (ref. 2) supports the conclusion of ref. 1. What is lacking is a set of data from a rotating system which is of sufficient detail as to make careful local comparisons between static cascade and rotor blade heat transfer. In addition, data is needed in a rotating system in which there is sufficient documentation of the flow field to support the computer analyses being developed today. Other important questions include the impact of both random and periodic unsteadiness on both the rotor and stator airfoil heat transfer. The random unsteadiness arises from stage inlet turbulence and wake generated turbulence and the periodic unsteadiness arises from blade passing effects. A final question is the influence, if any, of the first stator row and first stator inlet turbulence on the heat transfer of the second stator row after the flow has been passed through the rotor.

## OBJECTIVES

The first program objective is to obtain a detailed set of heat transfer coefficients along the midspan of a stator and a rotor in a rotating turbine stage (Fig 1.) These data are to be such that the rotor data can be compared directly with data taken in a static cascade. The data are to be compared to some standard analysis of blade boundary layer heat transfer which is in use today. In addition to providing this all-important comparison between rotating and stationary data, this experiment should provide important insight to the more elaborate full three-dimensional programs being proposed for future research. A second program objective is to obtain a detailed set of heat transfer coefficients along the midspan of a stator located in the wake of a full upstream turbine stage. Particular focus here is on the relative circumferential location of the first and second stators. Both program objectives will be carried out at two levels of inlet turbulence. The low level will be on the order of 1 percent, and the high level on the order of 10 percent, which is more typical of combustor exit turbulence intensity. The final program objective is to improve the analytical capability to predict the experimental data.

## PROGRESS

Heat transfer measurements will be obtained in this study using low conductivity rigid foam castings of the test airfoils. A uniform heat flux will be generated on the surface of the foam test airfoils using electrically heated metal foil strips attached to the model surface. Local heat transfer coefficients around the airfoils will be determined using thermocouples to measure the temperature difference between the heated metal skin and the free stream.

Photographs of the First Stage Rotor Model at various steps of fabrication are presented in Fig. 2. The first stage of the fabrication process consisted of developing a metal "master airfoil". An aluminum rotor blade, chosen at random from the Large Scale Rotating Rig (LSRR) rotor, was carefully inspected to determine locations with surface waviness. These slight deviations from a perfectly "developable" surface (a surface with no compound curvature) are an inherent characteristic of the "multiple radial station contour tracing" machining process used to manufacture the aluminum airfoils. Despite the fact that this surface waviness only consists of depressions a few thousandths of an inch deep at their maximum, they do present a problem unique to this method of instrumentation. The metal foil which will be glued to the exterior surface of the airfoil is extremely intolerant of surface waviness. Even miniscule depressions on the airfoil translate to "wrinkles" or "lumps" on the finished, assembled foil surface. For this reason it was necessary that any depressions be filled to produce as nearly a "developable" surface as possible. This filling procedure consisted of a trial-and-error/inspection iteration towards the finished airfoil. An airfoil was accepted as a "master" only after a completely wrinkle-free "test" metal foil could be glued to its entire surface. An inviscid flow computation of the velocity distribution around the finished "master" airfoil indicated that the maximum change in local velocity produced by the surface filling (measured maximum filling thickness) was only 1/4 percent. A photograph of the completed "metal master airfoil" is presented in Fig. 2.

The next step in the model fabrication process (not shown in Fig. 2) consisted of casting a concrete mold of the master airfoil. Special low shrinkage gypsum cement (USG Hydrocal) was used to produce a smooth airfoil surface and a precise geometrical reproduction.

A steel skeleton (Fig. 2.) was fabricated for each of the test airfoils to ensure adequate strength to endure both the aerodynamic and centrifugal forces of the test environment. The skeleton provided a secure location to attach the foam airfoil to either the rotor hub or the stator case. The photograph of the first stage rotor skeleton presented in Fig. 2. shows the attachment "button" for fastening the blade to the hub.

The rotor airfoil was cast in rigid foam with the steel skeleton mounted in the concrete mold. A special fixture ensures that the mounting button on the skeleton was precisely located at the same position relative to the concrete mold as was the button on the original "metal master

airfoil". Photographs of the suction and pressure surfaces of the cast foam rotor blade are shown in Fig. 2. For this particular model the suction surface was instrumented and the pressure surface was the "backside" through which the instrumentation was routed. The suction surface view shows the pattern of holes to be used for installation of thermocouples. The holes in the suction surface were evenly spaced at one inch increments at the midspan location for the demonstration test. The pressure surface view shows the trenches cut into that surface for routing of thermocouple leads, the copper buss bars for connecting to the foil skin and the electric power leads. The copper buss bars ensure that the voltage along each end of the foil strip is uniform, producing a uniform current over the entire foil surface.

The rate of heat transfer varies strongly with location near the leading edge of an airfoil. Measurement of these extreme gradients in heat transfer requires a dense grid of thermocouples in this region. In an attempt to obtain accurate measurements in the leading edge region for the present test airfoils, a new high density thermocouple installation technique has been assessed. Shown in Fig. 3. is a photograph of the leading edge array installed in this particular rotor model. The photograph shows the backside of the leading edge region of the foil before it was installed on the airfoil. Also shown are a specially fabricated template for accurately locating thermocouple beads and a thin "transfer template" which is shown attached directly to the backside of the foil. This "transfer template" was removed following the completion of the thermocouple installation. Shown in the photograph are 20 thermocouples located at 0.050 in. apart within an estimated accuracy of  $\pm 0.005$  in.

The next photograph of Fig. 3. shows the rotor model with the heater foil installed on the suction surface only. In this photograph the thermocouples have been welded to the backside of the heater foil and routed through the trenches to the support bottom. The third photograph of Fig. 3. shows the model with the foil attached to the pressure surface and connected to the buss bars. At this stage the instrumentation cavity was refilled with urethane foam to conform to the original pressure surface contour. The final photograph of Fig. 3. shows the completed test model coated with flat black paint. This paint coating ensures a uniform, known emissivity so that a slight ( $\approx 3$  percent) but accurate radiation correction can be incorporated into the data reduction routine.

A demonstration of the rotor heat transfer measurement technique has been successfully carried out. This test showed: (1) that the instrumented Urethane foam heat transfer models could survive the centrifugal loading in the rotating frame of reference, (2) that the instrumentation within the heat transfer model, and specifically the dense array of thermocouples around the leading edge, could survive the centrifugal loading, and finally (3) that the slip-ring unit provides a reliable and effectively noise-free method of acquiring thermocouple data in the rotating frame of reference. The actual test airfoils (first stator, rotor, and second stator) each have typically 95 thermocouple sites with 60 at midspan and 20 concentrated near the leading edge of each airfoil. The instrumentation diagram for the first stage rotor is shown in Figure 4 as an example.

## REFERENCES

1. Lokay, V.I., and Trushin, V.A.: Heat Transfer from the Gas and Flow-Passage Elements of a Rotating Gas Turbine. Heat Transfer - Soviet Research, Vol. 2., No. 4, July 1970.
2. Dunn, M.G., and Holt, J.L.: The Turbine Stage Heat Flux Measurements. Paper No. 82-1289, AIAA/ASME 18th Joint Propulsion Conference, 21-23, June 1982, Cleveland, Ohio.

## OBJECTIVES

- Turbine first stator and rotor heat transfer data
- Rotor-stator interaction ( $\Delta X$ )
- Free stream turbulence
- Comparison with cascade data
- Second stator heat transfer data
- Stator-stator interaction ( $\Delta \text{Circ}$ )
- Quasi-steady and/or unsteady boundary layer analysis

# TURBINE STAGE AT 15% AXIAL GAP

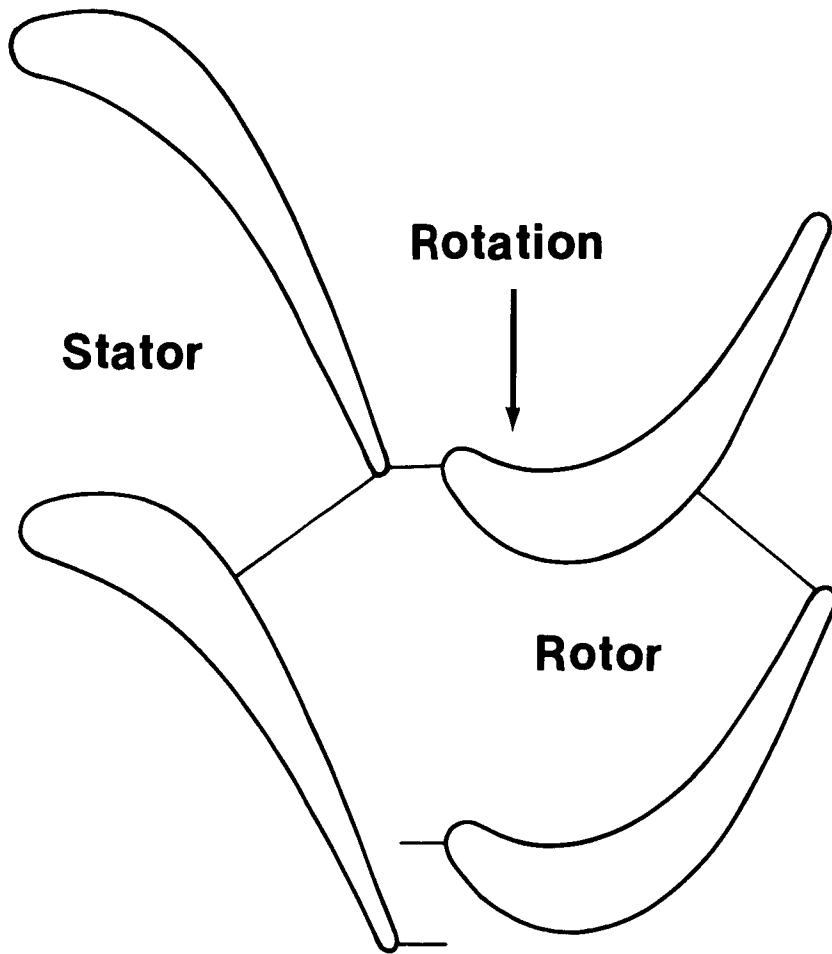
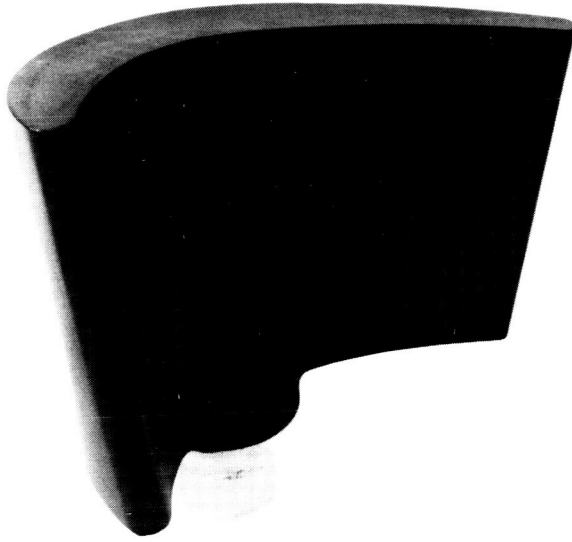


FIG. 1

ORIGINAL PAGE IS  
OF POOR QUALITY

STAGES OF FABRICATION FOR THE FIRST STAGE ROTOR



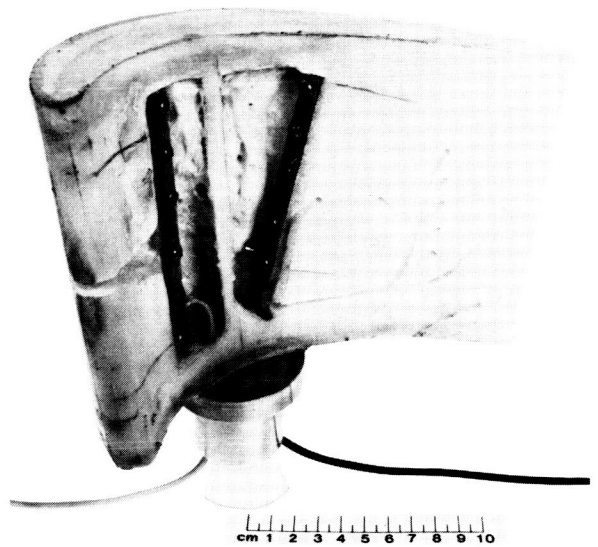
METAL MASTER AIRFOIL



STEEL SKELETON



SUCTION SURFACE OF CAST AIRFOIL



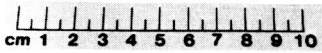
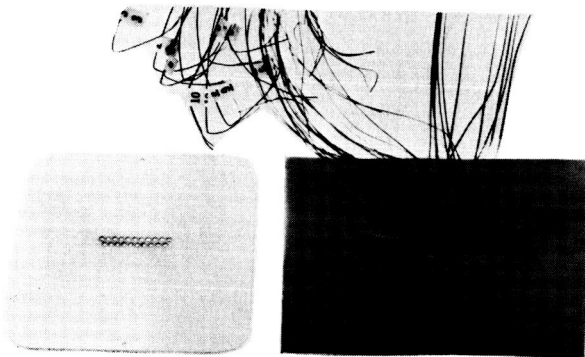
PRESSURE SURFACE OF CAST AIRFOIL

FIG 2

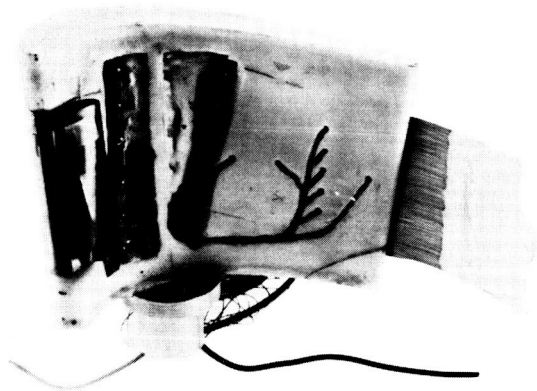
84-2-25-2

ORIGINAL PAGE IS  
OF POOR QUALITY

STAGES OF FABRICATION FOR THE FIRST STAGE ROTOR



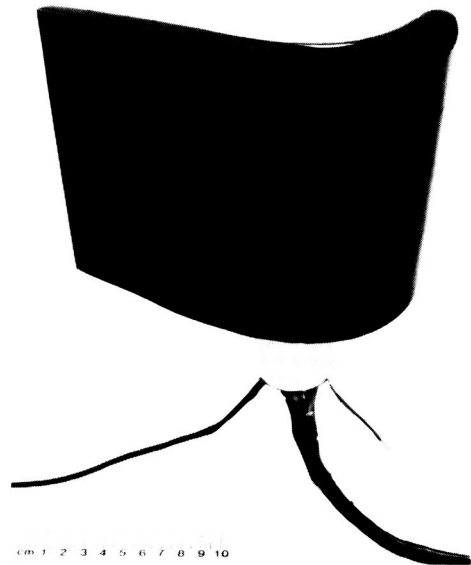
LEADING EDGE THERMOCOUPLE GRID



AIRFOIL WITH FOIL PARTIALLY INSTALLED



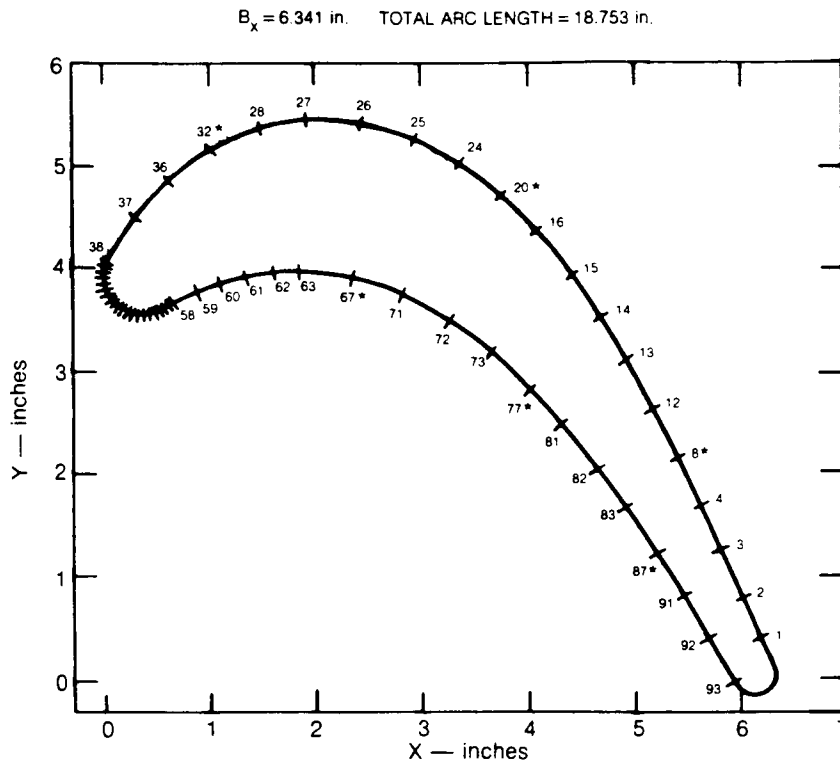
AIRFOIL WITH INSTRUMENTATION CAVITY CLOSED



COMPLETED TEST AIRFOIL

FIG. 3

INSTRUMENTATION DIAGRAM FOR THE FIRST STAGE ROTOR



NOTE — ORIGIN OF ARC LENGTH (S) IS THE AXIAL TRAILING EDGE  
(MAXIMUM X). S INCREASES MOVING COUNTERCLOCKWISE

SUCTION SURFACE AIRFOIL TC's 1-58  
PRESSURE SURFACE AIRFOIL TC's 38-93

TC #	$x/B_x$	$s/B_x$
1	0.975	0.065
2	0.945	0.148
3	0.912	0.227
4	0.878	0.306
8*	0.845	0.385
12	0.811	0.463
13	0.773	0.542
14	0.735	0.621
15	0.692	0.700
16	0.643	0.779
20*	0.588	0.858
24	0.525	0.936
25	0.456	1.015
26	0.382	1.094
27	0.303	1.173
28	0.226	1.252
32*	0.155	1.331
36	0.095	1.410
37	0.044	1.488
38	0.003	1.567

TC #	$x/B_x$	$s/B_x$
39	0.001	1.575
40	0.000	1.583
41	0.000	1.591
42	0.002	1.599
43	0.004	1.607
44	0.007	1.615
45	0.012	1.622
46	0.017	1.630
47	0.023	1.638
48	0.030	1.646
49	0.037	1.654
50	0.044	1.662
51	0.052	1.670
52	0.061	1.678
53	0.068	1.686
54	0.076	1.693
55	0.083	1.701
56	0.090	1.709
57	0.096	1.717
58	0.103	1.725

TC #	$x/B_x$	$s/B_x$
59	0.139	1.764
60	0.172	1.804
61	0.211	1.843
62	0.251	1.883
63	0.290	1.922
67*	0.371	2.000
71	0.445	2.080
72	0.513	2.159
73	0.574	2.237
77*	0.629	2.316
81	0.680	2.395
82	0.730	2.474
83	0.774	2.553
87*	0.820	2.632
91	0.858	2.711
92	0.899	2.789
93	0.940	2.868

\* AT THESE AXIAL STATIONS T.C.s LOCATED  
AT 50% SPAN AND  $\pm 8.3, 16.6$  AND 25%  
AWAY FROM MIDSPAN

FIG. 4